DEPARTMENT OF MATHEMATICS

Error Measurements for Semi-Lagrangian Schemes

C.J.Smith

Numerical Analysis Report 3/93

UNIVERSITY OF READING

Abstract

The semi-Lagrangian method is widely used in numerical weather models. The properties of the numerical solutions obtained by this method, depend strongly on the form of spatial interpolation used. In this report, several commonly used interpolants are reviewed and Fourier analysis is applied to the resulting schemes. rror measurements for the advection of more general data are then established, which build on the results of the Fourier analysis.

1.1	Lagrangian Description		3
1.2	Two T	Cime-Level Scheme	3
1.3	Interp	olation	5
	1.3.1	Lagrange Interpolation	5
	1.3.2	Hermite Cubic Interpolation	6
	1.3.3	Derivative stimates	7
	1.3.4	Cubic Spline Interpolation	7

n n

3.3	Conservation of 2nd Moment And Average Phase	rror	29
Conclu	sion		33

This report has two aims. The first is to describe the semi-Lagrangian method. This is an approach to the generation of finite difference schemes for problems involving advection. The importance of this method lies in the fact that it allows for some standard schemes are given for comparison.

1 The Semi-Lagrangian Method

The semi-Lagrangian method is a finite difference technique for the numerical modelling of advection, [8]. It achieves the redistribution, of a transported quantity, by solving local fluid trajectories over each time step. First it is necessary to consider the Lagrangian description of fluid flow. Following this, an overview of the two time-level semi-Lagrangian method is given.

1.1 Lagrangian Description

Let u(x,t) be some property of the fluid and let a(x,t) be the velocity field of the fluid. Passive transport of the quantity u is described by the one dimensional advection equation:

$$\frac{\partial u}{\partial t} + a \frac{\partial u}{\partial x} = 0. ag{1.1}$$

This equation may be written in terms of the Lagrangian (or convective) derivative,

$$-\frac{\partial}{\partial t} + a\frac{\partial}{\partial x},$$

when it becomes

$$\frac{u}{t} = 0. ag{1.2}$$

The Lagrangian derivative (1.2) provides the time rate of change, of the value of u, associated with any one particular fluid element. Such a fluid element is uniquely identified by specifying its position, x, at some reference time, t_{ref} . If $y(x, t_{ref}; t)$ is the position of this fluid element at time t, then the trajectory of the element is given by the equation,

$$\frac{dy}{dt} = a(y, t). (1.3)$$

1.2 Two Time-Level Scheme

The finite difference solution of (1.2) is to be established on an ulerian mesh with uniform space and time intervals, $\triangle x$ and $\triangle t$ respectively. Grid nodes are

at the positions $x_j = j \triangle x$ and the solution is to be advanced through successive time intervals, $t_n = n \triangle t$ where $n = 0, 1, 2, \cdots$.

Let U(x,t) be an approximate solution of (1.2) obtained numerically. If U is known up to the time level t_n , then it is advanced to the next time level using a discretization of (1.2). For a two time-level scheme [1] this discretization is

$$\frac{U(x_j, t_{n+1}) - U(y(x_j, t_{n+1}; t_n), t_n)}{\triangle t} = 0.$$
 (1.4)

where $y(x_j, t_{n+1}; t_n)$ is the position of the fluid trajectory at time t_n , described below. So at time t_{n+1} the value of U at the grid node x_j is given by

$$U(x_j, t_{n+1}) = U(y(x_j, t_{n+1}; t_n), t_n).$$
(1.5)

This important equation is the basic statement of the semi-Lagrangian method.

quation (1.2) states that, for any chosen fluid element, the value of u does not change with time. quation (1.5) is the discrete equivalent of this: the value of U held by the fluid element at (x_j, t_{n+1}) is exactly that which it held at the earlier time t_n . In order to find this value of U, it is first necessary to discover the position, $y(x_j, t_{n+1}; t_n)$, of the particle at time t_n . This position is known as the upstream departure point. It is found by performing an integration of the trajectory equation (1.3).

The simplest choice of integration is the uler method. For this particular problem it takes the form,

$$\frac{y(x_j, t_{n+1}; t_{n+1}) - y(x_j, t_{n+1}; t_n)}{\triangle t} = a(y(x_j, t_{n+1}; t_{n+1}), t_n). \tag{1.6}$$

Using the identity,

$$y(x_j, t_{n+1}; t_{n+1}) = x_j,$$

equation (1.6) results in the displacement formula:

$$y(x_j, t_{n+1}; t_n) = x_j - \triangle t \ a(x_j, t_n).$$

In practice the uler method is considered too inaccurate, but ordinary differential equation solvers of higher order can be applied to (1.3) in an entirely analogous way, [8].

The upstream departure point, once found, will generally not coincide with a grid node. Yet it is only at the nodes that a finite difference solution exists. This raises the need for interpolation to evaluate $U(y, t_n)$.

A finite difference method provides values of the approximate solution U(x,t) only at grid nodes, x_j . To obtain a value between nodes, any form of interpolation might be used. If a polynomial interpolant is chosen, then the scheme falls into a class of schemes particularly well suited to analysis. These are the explicit polynomial schemes considered in the next section of this report. First a number of interpolation options of practical importance are considered here.

This is the simplest form of polynomial interpolation. A small subset of grid nodes is selected, which surround the point at which an interpolated value is required.

Assume that the upstream departure point, y, lies between nodes k-1 and k. That is

$$x_{k-1}$$
 y x_k .

Take a sample set of p nodes either side of the interval $[x_{k-1}, x_k]$:

$$p = x_{k-p}, x_{k-p+1}, \dots, x_{k+p-1}$$
.

Let $_{2p-1}$ be the unique polynomial of degree 2p-1 which interpolates the finite difference solution at all the points in $_{p}$. Let $u_{j}=U(x_{j},t_{n})$ and $u^{j}=U(x_{j},t_{n+1})$, then

$$_{2p-1}(k-p)$$
 $k+p-1$ $k-p$ $k+p-1$; $k+p-1$; $k+r$ r

where

$$r(k-p)$$
 $k+p-1;$ $= \begin{cases} p-1 \\ s=-p \\ s\neq r \end{cases}$ $k+s$ $k+r$ (1.7)

For a constant velocity field, the velocity is simply displacement over time,

$$= -\frac{j}{} \tag{1.8}$$

This provides the following useful formula for the Courant number:

$$--- = -\frac{j}{j}$$

The set $_p$ is centred on the interval $[_{k-1} _{k}]$, which contains the departure point . As a consequence always lies within one grid interval, $_{k}$, of $_{k}$. Now equation (1.7) indicates that the interpolation is built up of differences between $_{k}$ (and surrounding nodes) and $_{k}$. So if the Courant number is restricted to lie between 0 and 1, then there is no loss of generality putting $_{k}$ = $_{k}$ A further simplification of the equations results by remembering that $_{k}$ = $_{k}$ Redefining the polynomial in terms of the Courant number, it may now be written

where 0 1.

Only polynomials of degree 2—1 have been considered. ven degree polynomials are constructed in the same way. However it is not possible to centre the sample set about the upstream departure point: an even degree polynomial requires an odd number of data points. Stable schemes can still be constructed by choosing the sample set correctly. There are two possibilities of sample set for a second degree polynomial. Both lead to stable schemes. These are the uncon-

$$j$$
 j n

$$j-1/2$$
 $j = j-1$

The cubic spline is formed using approximations, c_j , for the second derivative at grid points [4]:

$$c_j \approx \frac{\partial^2 U}{\partial x^2}(x_j, t_n).$$

These derivative estimates are related to the finite difference solution by the formula,

$$\left(1 + \frac{1}{6}\delta^2\right)c_j = \frac{1}{\triangle x^2}\delta^2 u_j, \tag{1.9}$$

where $\delta^2 u_j = u_{j+1} - 2u_j + u_{j-1}$.

The cubic spline polynomial is

$$U(y, t_n) = S_3(\nu) \equiv -\Delta x^2 \frac{(c_j - c_{j-1})}{6} \nu^3 + \Delta x^2 \frac{c_j}{2} \nu^2$$

$$-\Delta x^2 \left[\Delta_{j-1/2} + \frac{1}{6} (2c_j + c_{j-1}) \right] \nu + u_j$$
(1.10)

1.3.5 Fourier Analysis of the Cubic Spline

As an example of the type of analysis used in this report, Fourier transforms are applied to equations (1.9) and (1.10). quation (1.9) involves the step operator E. The effect of the Fourier transform on this is to introduce the multiplicative factor $e^{-i\phi}$, where $\phi = k\triangle x$ and k is the independent variable of the transform.

Let \tilde{U} and \tilde{C} be the Fourier transforms of U and C, which are related by

$$\left(1 + \frac{1}{6}\delta^2\right)C(x, t_n) = \frac{1}{\triangle x^2} \delta^2 U(x, t_n).$$

The transform of this equation is

$$\tilde{C}\triangle x^2 = \lambda(\phi)\tilde{U}$$
 where $\lambda(\phi) = 6\left(1 - \frac{3}{2 + \cos\phi}\right)$.

A transform equation may be obtained for (1.10) in a similar way :

$$\tilde{U}(k, t_{n+1}) = g(\phi, \nu)\tilde{U}(k, t_n)$$
where
$$g(\phi, \nu) = -\frac{\lambda(\phi)}{6}(1 - e^{-i\phi})\nu^3 + \frac{\lambda(\phi)}{2}\nu^2$$

$$-\left[1 - e^{-i\phi} + \frac{\lambda(\phi)}{6}(2 + e^{-i\phi})\right]\nu + 1$$

2 Analysis of Finite Difference Schemes for Advection

2.1 Test Problem and its Discretization

In order to analyse the performance of a numerical solution scheme, a suitable test problem is required. This is usually taken to be the simplest differential equation whose solutions exhibit the process which is of interest. In the case of advection the following test problem is chosen:

$$\frac{\partial u}{\partial t} + a \frac{\partial u}{\partial x} = 0 \tag{2.11}$$

where u = u(x, t) and $a \ge 0$,

on the domain
$$\mathbf{D}$$
:
$$\begin{cases} -\infty & < x < \infty \\ t & \geq 0. \end{cases}$$

The choice of initial condition is dictated by the form of the analysis which is to be carried out. The simplest possibility is considered in section 2.4 and slightly more realistic data will be considered in section 2.5.

To establish a finite difference approximation for this problem, the domain must first be discretized. The following mesh, which is regular in both space and time, is used:

$$\mathbf{M}(\triangle x, \triangle t) = \left\{ (j \triangle x, n \triangle t) : j \in \mathbf{Z}, n \in \mathbf{N} \right\},\,$$

where $\triangle x$ and $\triangle t$ are the space and time grid intervals respectively. Now let

$$x_j = j \triangle x$$
 and $t_n = n \triangle t$, (2.12)

and let u_j^n be the finite difference solution at the mesh point (x_j, t_n) . That is,

$$u_j^n \approx u(x_j, t_n). \tag{2.13}$$

The time evolution of the finite difference solution is governed by a numerical scheme, which is obtained from some consistent discretization of the equation (2.11). One class of schemes will be considered.

The schemes of this class have the general form,

$$_{j}^{n+1} = \left(\right) \quad _{j}^{n} \tag{2.14}$$

where

aralone. PVzffOzW GAVe

j j+1

rs

j n

j n j n

where the last line follows from = —. Using the space step operator , the above may be written,

$$(j \quad n \quad 0) = ^{-\nu} (j \quad n \quad 0)$$

$$= ^{-\nu} (j \quad n) \quad (2.17)$$

where the final line is obtained from the analytical solution (2.16). Hence the evolution equation for the exact solution of (2.11) is

$$\begin{pmatrix} j & n + \end{pmatrix} = \begin{pmatrix} -\nu & \begin{pmatrix} j & n \end{pmatrix} \end{pmatrix} \tag{2.18}$$

This equation identifies the evolution operator for the exact solution, on the mesh : $^{-\nu}$. It corresponds to linear wave motion; during one time step, it shifts the solution through a distance determined by the mesh velocity . The evolution

ikx

0 ikx_j

For the above initial data the exact solution of (2.11) is a sinusoidal progressive wave. Such a wave is precisely specified by just two parameters (the wavenumber k and the wave velocity a) and takes the form

$$u(x,t) = e^{ik(x-at)}.$$

If this solution is restricted to the mesh $\mathbf{M}(\triangle x, \triangle t)$, then the relevant parameters are the mesh dependent counterparts of k and a, that is ϕ and ν :

$$u(x_j, t_n) = e^{i\phi(j-\nu n)}. (2.20)$$

The space and time parts of this solution are separable allowing the solution to be written as

$$u(x_j, t_n) = (e^{-i\nu\phi})^n e^{ij\phi}.$$
 (2.21)

The quantity $e^{-i\nu\phi}$ is the amplification factor for the exact solution. It is obtained by the action of the exact evolution operator, $E^{-\nu}$, on the Fourier wave $e^{i\phi}$:

$$E^{-\nu}e^{i\phi} = e^{i(1-\nu)\phi} = e^{-i\nu\phi} e^{i\phi}.$$

The parameters ϕ and ν also determine the finite difference solution. They enter the solution through the action of the evolution operator, $C(E, \nu)$ as follows. Using (2.14) and (2.19) the solution after the first time step is

$$u_i^1 = \mathcal{C}(E, \nu) e^{ij\phi}.$$

This may be expanded using (2.15),

$$C(E, \nu) e^{ij\phi} = \sum_{r} c_r(\nu) E^r e^{ij\phi}$$

$$= \sum_{r} c_r(\nu) e^{i(j+r)\phi}$$

$$= e^{ij\phi} \sum_{r} c_r(\nu) e^{ir\phi}.$$

The summation in the last line may be written in terms of the polynomial C, which leads to

$$u_i^1 = e^{ij\phi} \ \mathcal{C}(e^{i\phi}, \nu).$$

-		
-		
	-	
		

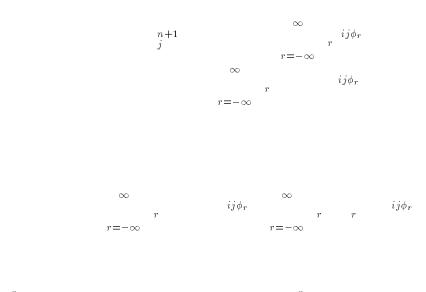
So far only waves composed of a single frequency have been considered. A more realistic approach is to consider the advection of a periodic wave, which contains a superposition of frequencies. (For instance the initial data may be chosen to be a square or triangular wave.) This allows the possibility of analysing such phenomena as dispersion and frequency dependent attenuation. However the approach which will be made here, is to look for measurements of amplitude and phase error averaged over all frequency components.

At time _n, let the data take the form

$$\int_{j}^{n} = \int_{r=-\infty}^{\infty} r(n)^{-ij\phi_{r}}$$
(2.26)

where $_r$ are the Fourier weights and $_r$ the wave numbers of the component Fourier modes.

When the solution is advanced one time step using (2.14), the linearity of the scheme results in each Fourier mode being separately advected:



The chosen measure of phase error is simply a weighted sum of the phase errors for each Fourier component:

$${}_{n}(\nu)^{2} = \frac{|\alpha_{r}(t_{n})|^{2} \left\{ \arg[g(\phi_{r}, \nu)] - (-\nu\phi_{r}) \right\}^{2}}{\sum_{r=-\infty}^{\infty} |\alpha_{r}(t_{n})|^{2}}.$$
 (2.27)

The corresponding weighted amplitude error would appear to be of little use; it is symmetric about the stability limit |g| = 1. However, by making use of Parseval's Theorem, the conserved fraction (defined below) of the second moment of the solution may be obtained.

Consider an infinite periodic wave with wavelength 2l:

If
$$f(x) = \int_{r=-\infty}^{\infty} \alpha_r e^{ir\pi x/l}$$
then
$$\frac{1}{2l} \int_{-l}^{l} f(x)^2 dx = \int_{r=-\infty}^{\infty} |\alpha_r|^2$$

under suitable conditions on f(x).

Let $U(x, t_n)$ be the continuous extension of the finite difference solution, where the index j is replaced by $x/\Delta x$:

$$U(x,t_n) = \int_{r=-\infty}^{\infty} \alpha_r(t_n) e^{i\phi_r x/\Delta x}$$
 (2.28)

and let

$$M_n = \int_{-L}^{L} U(x, t_n)^2 dx.$$

If the wavelength is 2L then Parseval's Theorem provides the following:

$$M_n = 2L \int_{r=-\infty}^{\infty} |\alpha_r|^2.$$
 (2.29)

When the evolution operator $C(E, \nu)$ is applied to (2.28), each Fourier mode produces an amplification factor:

$$U(x, t_n + \triangle t) = \int_{r=-\infty}^{\infty} \alpha_r \ g(\phi_r, \nu) \ e^{i\phi_r x/\triangle x}.$$

Applying Parseval's Theorem to this gives

$$M_{n+1} = 2L \sum_{r=-\infty}^{\infty} |\alpha_r \ g(\phi_r, \nu)|^2.$$
 (2.30)

Define the conservation fraction per time step for the second moment:

$$C_n(\nu) = \frac{M_{n+1}}{M_n}$$

From (2.29) and (2.30) this is seen to be

$$C_{n}(\nu) = \frac{\sum_{r=-\infty}^{\infty} |\alpha_{r}(t_{n})|^{2} |g(\phi_{r}, \nu)|^{2}}{\sum_{r=-\infty}^{\infty} |\alpha_{r}(t_{n})|^{2}}.$$
(2.31)

For linear advection with a constant velocity field, all the finite difference schemes considered in this report provide perfect conservation of mass. The second moment is not necessarily conserved: non-conservation is a result - though not a necessary one - of changes in the shape of the advected mass distribution.

2.5.4 Convergence of $\mathbf{E}_n(\nu)$ and $\mathbf{C}_n(\nu)$

Convergence of the summations in (2.27) and (2.31) follows from a property of the Fourier expansion, namely, that $\sum |\alpha_r|$ converges. Convergence of C_n is ensured since $|g| \leq 1$, for any stable scheme.

There is a slight problem involved in the calculation of $_n(\nu)$. Care must be taken in the calculation of $\arg[g(\phi_r,\nu)] + \nu\phi_r$, which is the phase error in the amplification factor for Fourier mode $e^{i\phi_r}$. The problem arises when $\nu\phi_r$ is outside the range of the arg function, since it is then necessary to find the winding number for $g(\phi_r,\nu)$. However, this may be side-stepped by recalling that waves with wavenumbers ϕ and $\phi + 2\pi$ are indistinguishable on the grid. This allows the phase error to be mapped onto the interval $(-\pi,\pi]$ by the addition/subtraction of multiples of 2π . Provided the scheme is known never to produce phase errors exceeding 2π , then the above procedure provides the correct phase error. This is the case for all the schemes to be considered here.

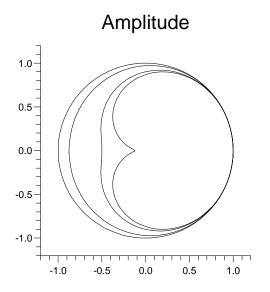
2.5.5 Courant Average

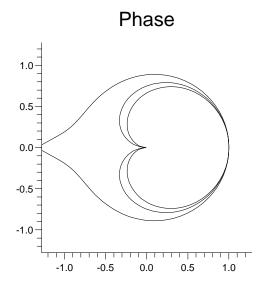
By averaging $C_n(\nu)$ and $n(\nu)$ over the range $0 \le \nu \le 1$, single values are obtained, corresponding to second moment conservation and average phase error respectively. This is accomplished by dividing the unit ν -interval into N equal parts. Define

$$\overline{C}_n = \frac{1}{N} \sum_{r=0}^{N} C_n(r/N)$$

$$-_n = \frac{1}{N} \sum_{r=0}^{N} {}_n(r/N).$$

Finally, we have arrived at two quantities related to the error in numerically advecting an arbitrary periodic wave. Both quantities are time dependent. This is due to the relative changes in the Fourier coefficients, since they each evolve according to their own amplification factor. Unlike the single Fourier wave case, where the wave retains similarity of form throughout all time steps, the data now changes its shape. Since it is the finite difference scheme which causes this change, it is to be expected that the scheme will perform better for this new shape: the shape becomes better suited to the scheme. This indicates that measurements of the error committed during the first time step are sufficient to describe the scheme's performance. It is then only a matter of testing the scheme with a variety of different initial wave shapes. The values of \overline{C}_0 and $\overline{}_0$ then indicate the scheme's effectiveness for the chosen shape.





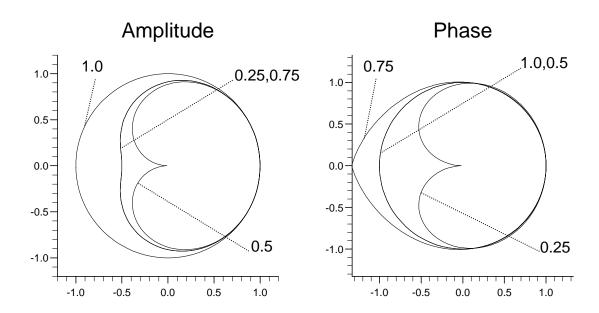


Figure 4: Fromm's Scheme

3.2 Semi-Lagrangian Schemes

In section 1 the semi-Lagrangian finite difference method was presented, along with several possible choices for interpolation. The results of Fourier analysis on these schemes is presented here in graphical form.

Cubic Lagrange The Lagrange interpolating polynomial of degree three is the simplest semi-Lagrangian method with fourth order spatial accuracy.

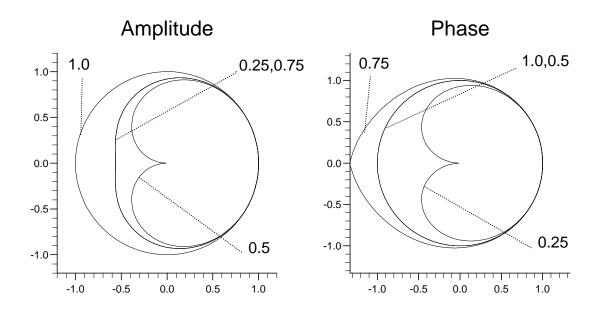


Figure 5: Cubic Lagrange

Quintic Lagrange Despite the extra effort in computing a higher degree polynomial, the quintic Lagrange method shows little improvement over the cubic Lagrange.

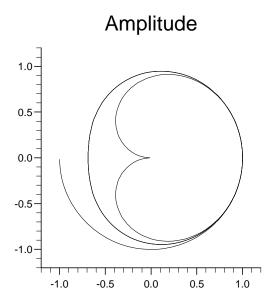
Hermite Cubic with Arithmetic Mean Hermite cubic interpolation requires estimates for the derivative at each grid node. These are usually expressed in terms of the discrete slopes of the finite difference solution. A simple form of

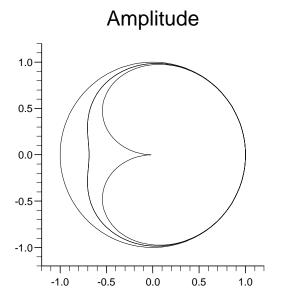
derivative estimate is provided by the mean of the discrete slopes, either side of a grid node.

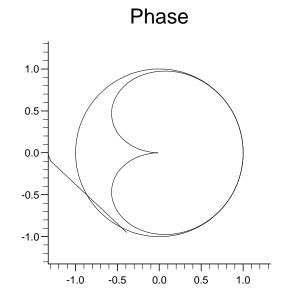
Hermite Cubic with Priestley Derivatives The Priestley derivative estimate [6] provides fourth order accuracy. This is consistent with the accuracy of the Hermite cubic itself.

Hermite Cubic with Hyman Derivatives The Hyman derivative estimate
[3] is similar in form to Priestley's.

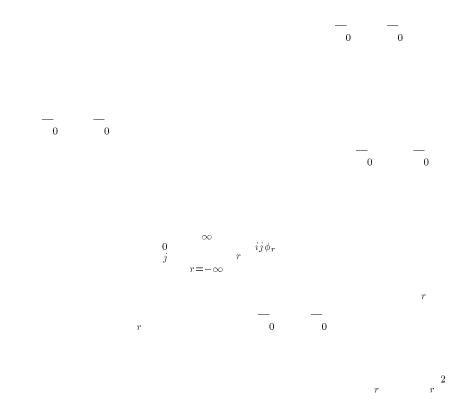
Cubic Spline This is a global interpolation method requiring considerable computational effort when used in practice.

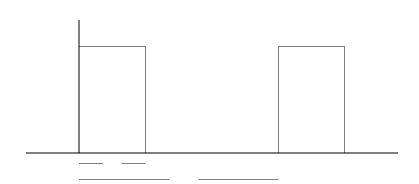






In section 2.5 the errors incurred by numerically advecting an arbitrary periodic





The component wave numbers are

$$\phi_r = r\pi \frac{\triangle x}{l}.$$

where $r = 0, \pm 1, \pm 2, \cdots$.

The corresponding error weights are

$$|\alpha_0|^2 = \left(\frac{\mu}{2}\right)^2$$

$$|\alpha_r|^2 = \frac{\sin^2(r\pi\mu/2)}{(r\pi)^2}$$

where $r = \pm 1, \pm 2, \cdots$.

Saw-Tooth Wave The saw-tooth wave, with wavelength 2l, is shown in figure 12.

This has component wave numbers

$$\phi_{2r} = 0$$

$$\phi_{2r+1} = (2r+1)\pi \frac{\triangle x}{l}$$

where $r = 0, \pm 1, \pm 2, \cdots$

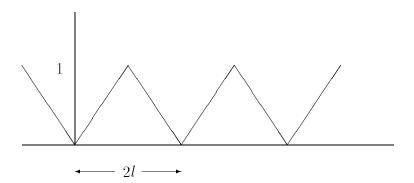


Figure 12: Saw-Tooth

The corresponding weights are

$$|\alpha_0|^2 = \frac{\pi^2}{4}$$

$$|\alpha_{2r}|^2 = 0 \qquad r = \pm 1, \pm 2, \cdots$$

$$|\alpha_{2r+1}|^2 = \frac{4}{\pi^2 (2r+1)^4} \quad r = 0, \pm 1, \pm 2, \cdots$$

Parabolic Blips This test wave is similar to the square wave described above, except that the square waves are replaced by parabolas. The wave is described by the function:

$$f(x) = \begin{cases} \frac{4}{l^2} x(l-x) & 0 \le x < l \\ 0 & l \le x < 2l \end{cases}$$

where $f(x \pm 2l) = f(x)$. The wave numbers and corresponding weights which this function gives rise to are:

$$\phi_0 = 0$$

$$\phi_r = r\pi \frac{\triangle x}{I}$$

and

$$|\alpha_0|^2 = \left(\frac{1}{3}\right)^2$$

$$|\alpha_{2r-1}|^2 = \left[\frac{8}{\pi^3 (2r-1)^3}\right]^2$$

$$|\alpha_{2r}|^2 = \left(\frac{1}{\pi^2 r^2}\right)^2$$

where $r = 1, 2, \cdots$

The measure of conservation of second moment is an absolute quantity: \overline{C}_0 takes the value 1 if the second moment is conserved exactly; above and below this value correspond to gain and loss respectively. This is not the case for the phase measure, $\overline{}_0$. It takes the value 0 if there is no phase error. However no scale has yet been defined for non-zero values. It is chosen here to assign a phase error of 1 to the first order upwind scheme, and scale the errors for other schemes accordingly.

For each of the test waves there is a parameter which must be specified. This is the quantity —. It describes how well the wave is represented on the grid: it is the ratio of the grid spacing to a half wavelength. When this parameter is varied,

	 	 	0

The weighted averages for phase error and second moment conservation error ap-

${\bf Acknowledgements}$

I would like to thank Dr. M.J. Baines and Dr. A. Priestley for suggesting the work reviewed here, and for their continual guidance throughout. I acknowledge receipt of an S-RC/Meteorological Office CAS—Award.

References

- [1] Bates J.R. and McDonald A. (1982) Multiple Upstream, semi-Lagrangian Advective Schemes Analysis and Application to a Multi-Level Primitive Equation Model. Mon. Wea. Rev. 112,2033-2047.
- [2] Fromm J. . (1968) A Method for Reducing Dispersion in Convective Difference Schemes. J. Comp. Phys. **3**,176-189.
- [3] Hyman J.M. (1983) Accurate Monotonicity Preserving Cubic Interpolations. SIAM J. Sci. Stat. Comp. 4,645-654.
- [4] Jacques I. and Judd C. (1987) Numerical Analysis. Chapman and Hall.
- [5] Lax P.D. and Wendroff B. (1960) Systems of Conservation Laws. Comm.Pure and Appl. Math. X,537-566.
- [6] Priestley A. (1993) To appear, J. Comp. Phys.
- [7] Rasch P.J. and Williamson D.L. (1990) On Shape-Preserving Interpolation and Semi-Lagrangian Transport. SIAM J. Sci. Stat. Comp. 11,656-689.
- [8] Staniforth A. and Côté J. (1991) Semi-Lagrangian Integration Schemes for Atmospheric Models Review. Mon. Wea. Rev. 119,2206-2223.
- [9] Temperton C. and Staniforth A. (1987) An Efficient Two-Time Level Semi-Lagrangian Semi-Implicit Integration Scheme. Q.J.R. Met. Soc. 113,1025-1039.
- [10] Warming R.F. and Beam R.W. (1976) Upwind Second-Order Difference Schemes and Applications in Aerodynamic Flows. AIAA J. 24,1241.